Parameter Estimation/Sensitivity Analysis for an Aquifer Test with Skin Effect

by Yen-Ju Chen[1] and Hund-Der Yeh[2]

Abstract

Aquifer information carried by aquifer test data may be affected by the presence of a finite thickness skin around the wellbore. The mathematical treatment for an aquifer accounting for the skin zone can be characterized by five parameters, that is, the outer radius of the skin zone and the transmissivity and storativity for each of the skin and aquifer zones. Sensitivity analysis was performed to examine the ground water flow behavior in the skin and aquifer zones in terms of the constant-head test (CHT) data. The simulated annealing procedure was applied to simultaneously determine the skin and aquifer parameters from the analysis of CHT data. Toward the previously mentioned goals, four suites of CHT data were analyzed in this article. The analyses of wellbore flow rate at the test well and the specific drawdown at the observation well gave accurate estimates for the skin and aquifer parameters, respectively. Only the skin thickness and both the skin and the aquifer diffusivities could be accurately estimated from the analysis of drawdown data in the observation well. The estimates for all skin and aquifer parameters from the composite analysis of flow rate and drawdown data were the most accurate. The results of sensitivity analyses and parameter estimations provide instructive references in the analysis of the skin-affected CHT data.

Introduction

In a constant-head test (CHT), the buildup or drawdown in the test well is kept constant throughout the test, and the transient flow rate at a test well or dispensable buildup/(drawdown) in an observation well is measured. The aquifer parameters such as transmissivity and storativity may then be determined from the analysis of these measurements. Jacob and Lohman (1952) derived the flow rate solution for a CHT conducted on a fully penetrating well in a confined aquifer. They indicated that

both CHT and constant-flux test (CFT) drawdown solutions are identical at sufficiently large time. The specific drawdowns, that is, the drawdown divided by the wellbore flow rate of CHT and CFT, therefore are equivalent at sufficiently large time. The late-time specific drawdown data of CHT can be analyzed for determining aquifer transmissivity and storativity based on the Theis (1935) type-curve method or Cooper and Jacob's (1946) method. Mishra and Guyonnet (1992) used the specific drawdown in the observation well to determine the aquifer parameters during the CHT. Both the Theis (1935) type-curve method and Cooper and Jacob's (1946) method were applied in their study. Based on the late-time approximate solution proposed by Hantush (1964), Hiller and Levy (1994) showed that only the hydraulic diffusivity can be determined from the analysis of the drawdown data.

Well drilling or completion may cause disturbance to the near wellbore aquifer and thus produce a skin zone with diverse properties to the aquifer. The skin can be classified into two categories: a positive skin (also called

[1]Institute of Environmental Engineering, National Chiao Tung University, 75 Po-Ai Street, Hsinchu 30039, Taiwan; yenju.ev92g@nctu.edu.tw
[2]Corresponding author: Institute of Environmental Engineering, National Chiao Tung University, 75 Po-Ai Street, Hsinchu 30039, Taiwan; 886-3-5731910; fax: 886-3-5726050; hdyeh@mail.nctu.edu.tw
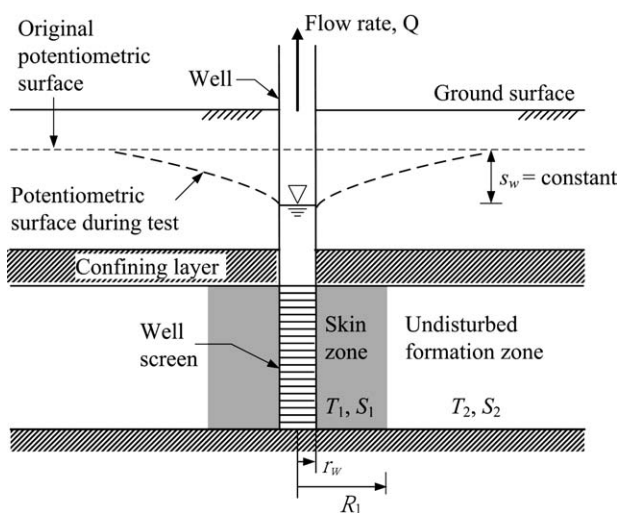
a low-permeability skin) having a smaller value of transmissivity than the aquifer zone and a negative skin (also called a high-permeability skin) having a larger value of transmissivity than the aquifer zone. The presence of the skin zone may influence the estimation of hydrogeological properties from the analysis of the observed data. Chen and Chang (2003) indicated that both the observation well drawdown and the test well flow rate should be included if a CHT is affected by infinitesimal skin. With the presence of finite thickness skin, the aquifer becomes a radial two-zone system characterized by the five parameters, namely the outer radius of the skin zone and the transmissivity and storativity for each of the skin and aquifer zones as shown in Figure 1. Yang and Yeh (2002) developed the time-domain solution for the transient flow rate at the test well in a two-zone aquifer system by using the Laplace transforms and the Bromwich integral method. The extended work presented in Yang and Yeh (2005) can simulate the transient flow rate and hydraulic head distribution when a CHT is conducted on a partially penetrating well.

Determination of the skin and aquifer parameters from the analysis of measured data is a subject of inverse problem and can be cast as an optimization problem. Different from the manual type-curve matching, the simulated annealing (SA) algorithm is chosen as the optimization strategy to determine the skin and aquifer parameters so that the predicted results closely match the measured data. The SA algorithm was first proposed by Metropolis et al. (1953) in computer simulation of material configuration. Later, Kirkpatrick et al. (1983) introduced the concept of Metropolis et al. (1953) to combinatorial optimization. Nowadays, the use of SA to solve an optimization problem has been successfully applied in water resources area. For example, the method has been used to plan the strategies of ground water remediation (Dougherty and Marryott 1991; Marryott et al. 1993), predict trihalomethane species in chlorinated water (Lin and Yeh, 2005), design the optimal network or water resource conservation (e.g., Cunha and Sousa 1999; Kuo et al. 2001; Yeh and Lin 2008), and identify the aquifer parameters (e.g., Zheng and Wang 1996; Chang et al. 2008).

Sensitivity analysis, which investigates the model response to the perturbations in the parameters, is important in terms of parameter estimation (McElwee and Yukler 1978; Jiao and Rushton 1995; Huang and Yeh 2007). The model response is insensitive to a specific parameter when the perturbation in that parameter has little impact on the output. It is hard to determine an insensitive parameter due to wide-ranged values of that parameter producing similar output data. High-correlated sensitivtity features between parameters also cause difficulty in parameter estimation because the model responses affected by one parameter might be shadowed by another.

The main objective of this article is to investigate the ground water flow behavior affected by a finite thickness skin and to extract skin and aquifer parameter information behind the CHT data from the viewpoint of sensitivity analysis. Another objective is to determine the skin and aquifer parameters synchronously from the analyses of CHT data under the condition of a finite thickness wellbore skin. The methodology of parameter estimation used in this study has been successfully applied to the problem for a slug test with wellbore skin (Yeh and Chen 2007). We further assess the feasibility of using CHT data to estimate skin and aquifer parameters fitted to Yang and Yeh's (2002) solution. The study primarily assumed a CHT conducted on a fully penetrating well in a confined aquifer with a finite thickness skin. Toward our goals, four suites of CHT data were analyzed, which comprises the wellbore flow rate at the test well, drawdown in an observation well, the specific drawdown at the observation well, and composite analysis of flow rate and drawdown data.

Data Analysis Methodology

Field Data Simulator

The closed-form solutions for the wellbore flow rate at the test well and drawdown in an observation well were developed by Yang and Yeh (2002) and Yang and Yeh (2006), respectively; yet, it is rather complicated to evaluate them directly (Peng et al. 2002; Yang and Yeh 2006). The Laplace-domain solutions as substitutes were used to simulate the field data. The mathematical model of Yang and Yeh (2002) can refer to Appendix A. They gave the flow rate solution in the Laplace domain when the CHT is conducted on a fully penetrating well in a confined aquifer with a finite thickness skin as follows:

$$\overline{Q}(p) = \frac{2\pi r_w T_1 s_w q_1 [\Phi_1 I_1(q_1 r_w) + \Phi_2 K_1(q_1 r_w)]}{p[\Phi_2 K_0(q_1 r_w) - \Phi_1 I_0(q_1 r_w)]} \quad (1)$$

with variables Φ_1 and Φ_2, respectively, defined as follows:

Figure 1. Schematic representation of a CHT conducted in a confined aquifer with a finite thickness skin.

$$\Phi_1 = \sqrt{\frac{S_2 T_2}{S_1 T_1}} K_0(q_1 R_1) K_1(q_2 R_1) - K_1(q_1 R_1) K_0(q_2 R_1) \tag{2}$$

and

$$\Phi_2 = \sqrt{\frac{S_2 T_2}{S_1 T_1}} I_0(q_1 R_1) K_1(q_2 R_1) + I_1(q_1 R_1) K_0(q_2 R_1) \tag{3}$$

where $\overline{Q}$ is the flow rate across the wellbore in the Laplace domain; p is the Laplace variable; r_w is the radius of well; s_w is the constant drawdown maintained at the well during the test; T and S are the transmissivity and storativity with the subscripts 1 and 2 representing the skin and aquifer zone, respectively; R_1 is the radial distance from centerline of the well to outer boundary of skin zone; $q_1 = \sqrt{pS_1/T_1}$; $q_2 = \sqrt{pS_2/T_2}$; I_0 and K_0 are the zero-order modified Bessel functions of the first and second kinds, respectively; and I_1 and K_1 are the first-order modified Bessel functions of the first and second kinds, respectively. The notation is given in Appendix B.

The drawdown solution in the Laplace domain is the same as the hydraulic head solution given by Yang and Yeh (2002):

$$\overline{s}_1(r,p) = \frac{s_w[\Phi_1 I_0(q_1 r) - \Phi_2 K_0(q_1 r)]}{p[\Phi_1 I_0(q_1 r_w) - \Phi_2 K_0(q_1 r_w)]} \tag{4}$$

or

$$\overline{s}_2(r,p) = \frac{s_w[\Phi_1 I_0(q_1 R_1) - \Phi_2 K_0(q_1 R_1)] K_0(q_2 r)}{p[\Phi_1 I_0(q_1 r_w) K_0(q_2 R_1) - \Phi_2 K_0(q_1 r_w) K_0(q_2 R_1)]} \tag{5}$$

where $\overline{s}_1$ and $\overline{s}_2$ describe the Laplace-domain drawdown responses in the skin and aquifer zones, respectively, and r denotes the location of the observation well. The numerical inversions of Equations 1, 4, and 5 to real time domain were obtained using the routine DINLAP of IMSL (2003a).

Sensitivity Analysis

Sensitivity analysis interprets the influence of input parameters (i.e., the five parameters) on output quantities (e.g., simulated flow rate, drawdown, or specific drawdown) of a model. For the sake of comparing parameters, which are in different unit and/or order of magnitude, the normalized sensitivity with respect to different parameters was expressed as follows (Kabala 2001):

$$X_{i,k} = P_k \frac{\partial O_i}{\partial P_k} \tag{6}$$

where $X_{i,k}$ is the normalized sensitivity of kth input parameter (P_k) at time i with the same unit as the output quantities (O_i). The partial derivative in Equation 6 can be approximated by the following finite-difference formula (Yeh 1987):

$$\frac{\partial O_i}{\partial P_k} = \frac{O_i(P_k + \Delta P_k) - O_i(P_k)}{\Delta P_k} \tag{7}$$

where ΔP_k denotes the small increment, which is approximated by $\Delta P_k = 10^{-3} P_k$ (Leng and Yeh 2003).

Parameter Estimation Method

The problem of determining the skin and aquifer parameters from measured field data can be categorized as an optimization problem. The definition of the objective function is contingent upon the type of field data being analyzed. Analysis of a specific field data set was formulated as a single-objective problem. Since r_w and s_w were known a priori, the five unknown parameters T_1, T_2, S_1, S_2, and R_1 were determined by:

$$f_k = \min_{\underline{p_e} \in \Omega} \sum_{i=1}^{n} (E_k(\underline{p_e}, t_i) - M_k(t_i))^2, \quad k = 1, 2, 3 \tag{8}$$

with

$$\underline{p_e} = \{p_e(T_1, T_2, S_1, S_2, R_1) | T_1 \in \Omega_1, T_2 \in \Omega_2,$$
$$S_1 \in \Omega_3, S_2 \in \Omega_4, R_1 \in \Omega_5\} \tag{9}$$

where f_k is the objective function defined as sum of squared residuals being minimized with the subscript k denoting three types of field data in the analysis, that is, flow rate, drawdown, and specific drawdown data for $k = 1$, 2, and 3, respectively; $\underline{p_e}$ is the unknown parameter vector; $\underline{\Omega}$ is the solution space with respect to $\underline{p_e}$; E_k and M_k are the kth type of predicted model output data and the kth type of measured field data at time t_i, respectively. The value of E_k can be determined by substituting a set of trial parameters into the corresponding solution, that is, Equations 1, 4, or 5. In addition, the composite analysis of the flow rate and drawdown data for the new objective function f_4 can be formulated as follows:

$$f_4 = \min_{\underline{p_e} \in \Omega} \left[w \times \sum_{i=1}^{n} [E_1(\underline{p_e}, t_i) - M_1(t_i)]^2 \right.$$
$$\left. + \sum_{i=1}^{n} [E_2(\underline{p_e}, t_i) - M_2(t_i)]^2 \right] \tag{10}$$

where w is a weight with the unit in d^2/m^4. Consider that the CHT is conducted in a low-permeability confined aquifer. Defining the appropriate searching ranges of the five parameters is helpful in saving the computer time (Yeh et al. 2007a). The physically appropriate ranges are generally made based on the field geology at the test site. The appropriate ranges for T_1 and T_2 were $\Omega_1 = \Omega_2 \in [0.01, 10]$ with the units both in m^2/d, and S_1 and S_2 were $\Omega_3 = \Omega_4 \in [10^{-5}, 10^{-3}]$. The R_1 was ranged by $\Omega_5 \in [0.1, 1]$ where the lower bound was selected as the well radius of 0.1 m.

SA algorithm was chosen to solve the optimization problem. This algorithm is developed based on the simulation of physical annealing process, where the objective

function is analogous to the free energy, and the solutions are analogous to the material states. The Metropolis criterion is the heart of SA algorithm, which describes the acceptance probability of moving from the current solution i to the trial solution j (Aarts and Korst 1989):

$$P(\text{accept trial solution } j)$$
$$= \begin{cases} 1 & \text{if} \quad f(j) \le f(i) \\ \exp\left(\dfrac{-[f(j)-f(i)]}{T}\right) & \text{if} \quad f(j) > f(i) \end{cases} \quad (11)$$

where T, the system temperature, is gradually reduced with an annealing schedule. The acceptance probability of an inferior solution will decrease with increasing system temperature. The SA procedure used in this study is similar to that described in Yeh and Chen (2007), and the required elements in the SA algorithm were listed as following:

1. The system had an initial temperature of 10.
2. The starting points of the five parameters were all chosen at their lower bound since the SA results are theoretically independent on the starting points (Yeh et al. 2007b).
3. The total number of iterations in each temperature level was taken as 500.
4. The annealing schedule for new temperature was generated by multiplying a cooling rate of 0.85 as suggested by Corana et al. (1987) and the old temperature.
5. The algorithm was terminated when either decrease in the best-so-far objective functions between two consecutive temperatures was less than 10^{-6} for four times sequentially or the number of total iterations reached 2×10^7 in the algorithm.

Scenarios Analyses and Results Discussion

Assume that a CHT was carried out in a silty confined aquifer. The fully penetrating well with 0.2-m diameter was maintained with a constant drawdown of 3 m during the test. The observation well was located at 1.2 m away from the test well. The target parameters chosen in the analyses were $T_1 = 0.05$ m²/d and $T_2 = 1.0$ m²/d for positive-skin cases, $T_1 = 1.0$ m²/d and $T_2 = 0.05$ m²/d for negative-skin cases, $S_1 = S_2 = 10^{-4}$, and $R_1 = 0.8$ m. Four suites of CHT data considered for the parameter estimations include the wellbore flow rate at the test well, drawdown at an observation well, the specific drawdown at the observation well, and the composite use of flow rate and drawdown data. The flow rate data were produced by Equation 1, and the drawdown data in the skin and formation zones were synthesized by Equations 4 and 5, respectively.

Sensitivity Analyses of Wellbore Flow Rate Data

Patterns of normalized sensitivities will change with different skin and aquifer parameters. A broad range of skin parameters were therefore examined in the sensitivity analyses. Figures 2a and 2b display the normalized
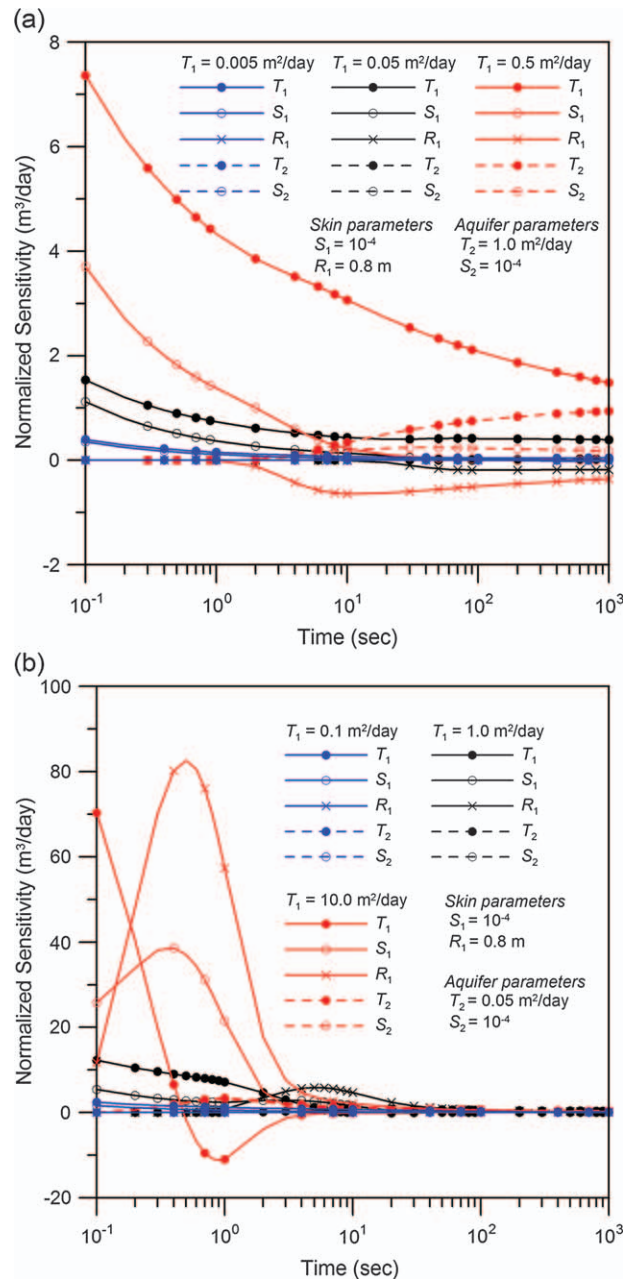
Figure 2. Normalized sensitivities of flow rate to the five parameters for different T_1 for the cases of (a) positive skin and (b) negative skin.

sensitivities of flow rate with respect to different T_1 for the positive- and negative-skin cases, respectively. The values of T_1 being examined were 0.005, 0.05, and 0.5 m²/d for the positive-skin cases and 0.1, 1, and 10 m²/d for the negative-skin cases. Figure 2a shows positive perturbations in the values of T_1 and S_1 resulting in positive influences on the flow rate at the wellbore, while that in R_1 negatively influence the flow rate. The influence of perturbation in S_1 on the flow rate vanishes at certain time since the skin zone storage responds to the test instantaneously. The magnitudes of normalized sensitivities to skin parameters T_1, S_1, and R_1 become smaller for a smaller T_1 in the positive-skin case. As for the negative-skin case, Figure 2b depicts that the increases in

skin parameters T_1, S_1, and R_1 appear to have positive influences on the flow rate at early time. The case of $T_1 = 10$ m^2/d is an exception in which the increase in T_1 results in positive influence on the flow rate before the first 0.4 s, and thereafter it produces negative influence on it. A larger T_1 and head difference between the well and the skin zone produce a larger amount of water flowing from the skin zone to the well at the beginning of the test. Yet, only a very small amount of water flows through the skin zone and toward the well because T_2 (0.05 m^2/d) is very small compared with T_1. Consequently, the head in the skin zone drops very quickly. The influence of T_1 on the flow rate also reduces very quickly and becomes negative as the time is increased. It is noteworthy that the increases in T_2 and S_2 in the case of $T_1 = 10$ m^2/d at early time produce apparent positive responses to the flow rate. At late time, the flow rate becomes insensitive to the changes in skin parameters; as a result, the use of early-time data seems favorable in estimating the skin parameters in the negative-skin case. Both Figures 2a and 2b show that the changes in skin parameters result in greater influences on the flow rate than those of aquifer parameters. Consequently, the determination of parameters from the analysis of wellbore flow rate data may result in more reliable skin parameters than aquifer ones. Figure 2 also shows that the magnitudes of normalized sensitivities of flow rate to the five parameters decrease with T_1 in both positive- and negative-skin cases. This implies that the smaller the transmissivity of skin zone, the more difficulty obtaining good estimate results.

Figures 3a and 3b exhibit how the normalized sensitivities of flow rate to the five parameters change with S_1 for the positive- and negative-skin cases, respectively. The values of S_1 being examined were 10^{-5}, 10^{-4}, and 10^{-3}. Figure 3 displays that the discrepancies in the normalized sensitivities of flow rate with different S_1 appear at early time. At early time, the magnitudes of normalized sensitivities of flow rate to T_1 and S_1 increase with S_1 because of more water taken from the skin zone storage. This means that the case with a larger S_1 may be more preferable in estimating the skin parameters. Later, the curves of normalized sensitivities to T_1 and S_1 for the cases of different S_1 are consistent. There is a time lag that the flow rate becomes sensitive to the change in R_1 in the case of large S_1. In addition, the maximum normalized sensitivities to R_1 also increase with S_1 in the negative-skin cases.

Figures 4a and 4b show the normalized sensitivities of flow rate to the five parameters with respect to different R_1 for the positive- and negative-skin cases, respectively. The values of R_1 being examined were 0.4, 0.8, and 1.2 m. For the positive-skin cases, Figure 4a shows the normalized sensitivity curves for different R_1 having the same patterns before the first 2 s. Thereafter, the magnitudes of normalized sensitivities of flow rate to T_1 and R_1 decrease with the increasing thickness of the skin zone. Figure 4b exhibits the patterns of normalized sensitivities to R_1, T_2, and S_2 shifted to the right in the time axis as R_1 is increased. The magnitude of normalized sensitivity to T_1 increases with R_1; in contrast, that to S_1

decreases at early time and increases at late time with the increasing R_1. Figures 4a and 4b both indicate that the flow rate is sensitive to the change in R_1 at later time as the skin zone becomes thicker. This suggests that longer flow rate data are preferred if R_1 is large in the positive-skin case. As indicated in Figures 2 through 4, the aquifer parameters may not be accurately estimated based on the flow rate data because the aquifer information may be overshadowed by the skin effect, especially in the positive-skin cases.

Parameter Estimation Using Flow Rate Data

The noise-free flow rate data at the test well at time t, $Q_{ub}(t)$, were generated by Equation 1. Taking account of the measurement errors, the observed flow rate data $Q_m(t)$ were considered as follows:

$$Q_m(t) = Q_{ub}(t) \cdot [1 + \varepsilon RN(o)] \qquad (12)$$

where ε denotes the error magnitude and is chosen to be 1% for representing the accuracy of flowmeter; $RN(o)$ symbolizes the random number on the order o corresponding to time t. Four sets of random numbers were applied and generated from a standard normal distribution by the routine RNNOF of IMSL (2003b).

Table 1 reveals the target values and estimated results of skin and aquifer parameters for scenarios 1 and 2, which, respectively, represent the positive- and negative-skin situations. Each scenario has five cases named cases a to e. The flow rate being analyzed in case a was directly generated using Equation 1, while those in cases b to e were synthesized using Equation 12 with four sets of random numbers. In addition, the standard error of estimate for the flow rate data (SEE$_Q$) (Yeh 1987) given in the rightmost column assesses the performance of parameter estimation, which is defined as follows:

$$\text{SEE}_Q = \sqrt{\frac{1}{v} \sum_{i=1}^{n} (E_1(t_i) - M_1(t_i))^2} \qquad (13)$$

where v is the degree of freedom that equals the number of measured data points minus the number of unknowns. The relative error (RE) given at the bottom row of Table 1 reflects the magnitude of parameter uncertainty on estimation and is calculated by taking mean value minus target value and then divided by the target one.

Scenario 1 gives accurate estimates for T_1, S_1, and R_1 with small RE of 0.32%, −0.91%, and 2.41%, respectively. The estimates of T_2 also have a small RE value of −7.80%; yet, the estimated values of the five cases are much dispersed based on the standard deviation of 0.235 m^2/d. The most inaccurate results happened to S_2 with a mean value of 6.36×10^{-4} and RE of 535.96%. The predicted flow rate based on the five estimated parameters is close to the measured flow rate according to the SEE$_Q$ values ranging from 3.19×10^{-3} to 9.05×10^{-3} m^3/d. For the negative-skin case, that is, scenario 2, all the estimated parameter values are fairly close to the target values as shown in Table 1, though the SEE$_Q$ values ranging
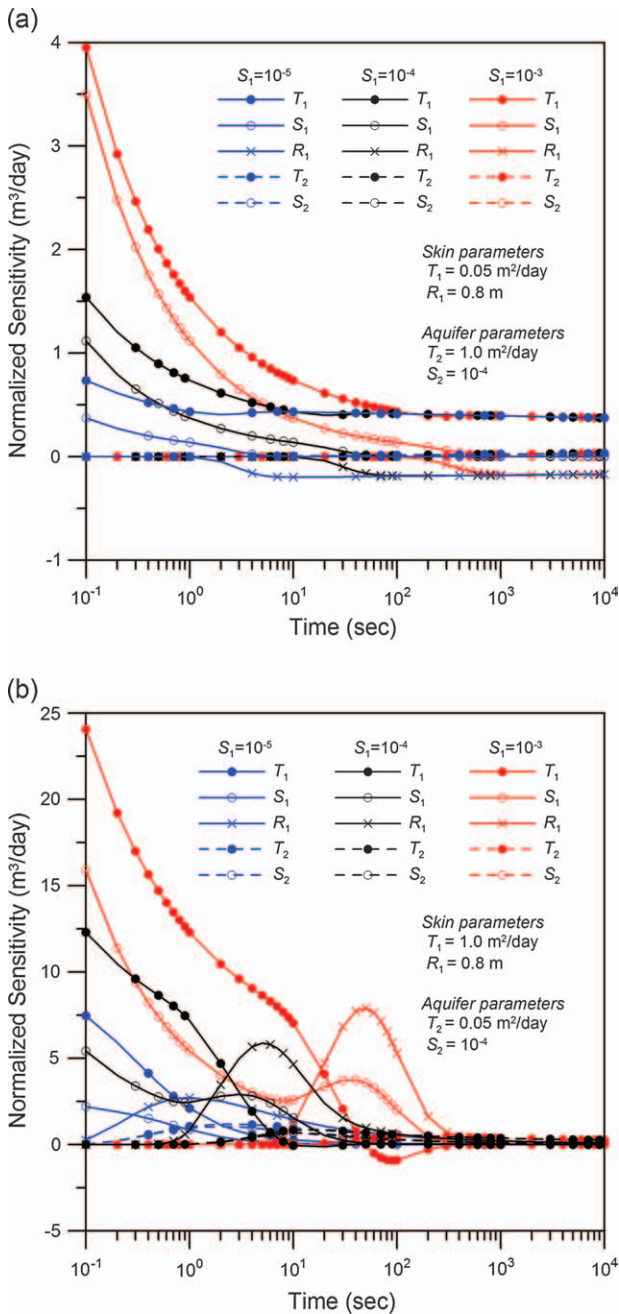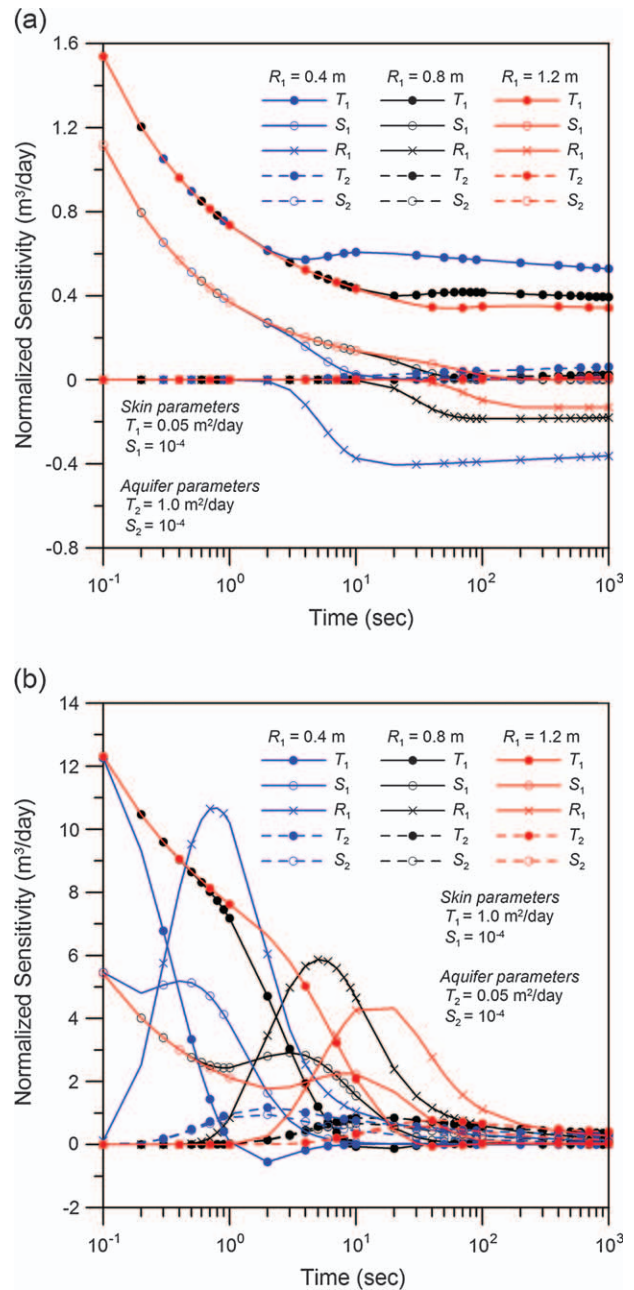
Figure 3. Normalized sensitivities of flow rate to the five parameters for different S_1 for the cases of (a) positive skin and (b) negative skin.

Figure 4. Normalized sensitivities of flow rate to the five parameters for different R_1 for the cases of (a) positive skin and (b) negative skin.

from 2.95×10^{-3} to 5.06×10^{-2} m³/d are slightly larger than those of scenario 1. The sensitivity analyses provide the clue why the estimate result for S_2 is inaccurate in scenario 1. This is because, as indicated in Figures 2 through 4, the flow rate data are almost insensitive to the changes in aquifer parameters, especially in the positive-skin cases.

Parameter Estimation and Sensitivity Analyses of Drawdown Data

The synthesized drawdown data in the observation well were analyzed. The noise-free drawdown data at the observation well at time t, $s_{ub}(t)$, are produced by Equation 5. The measured drawdown data $s_m(t)$ including the measurement errors may be expressed as follows:

$$s_m(t) = s_{ub}(t) + \varepsilon RN(o) \qquad (14)$$

where ε is chosen to be 0.001 for representing the accuracy of water level meter on the order of millimeters. Table 2 lists the target values and estimated results for skin and aquifer parameters from analyzing the measured drawdown data for aquifers with positive skin in scenario 3 and negative skin in scenario 4. The SEE_s values, the standard error of the estimated drawdown, given in the rightmost column were calculated using Equation 13

Table 1
Target Values and Estimated Results for Scenarios 1 and 2

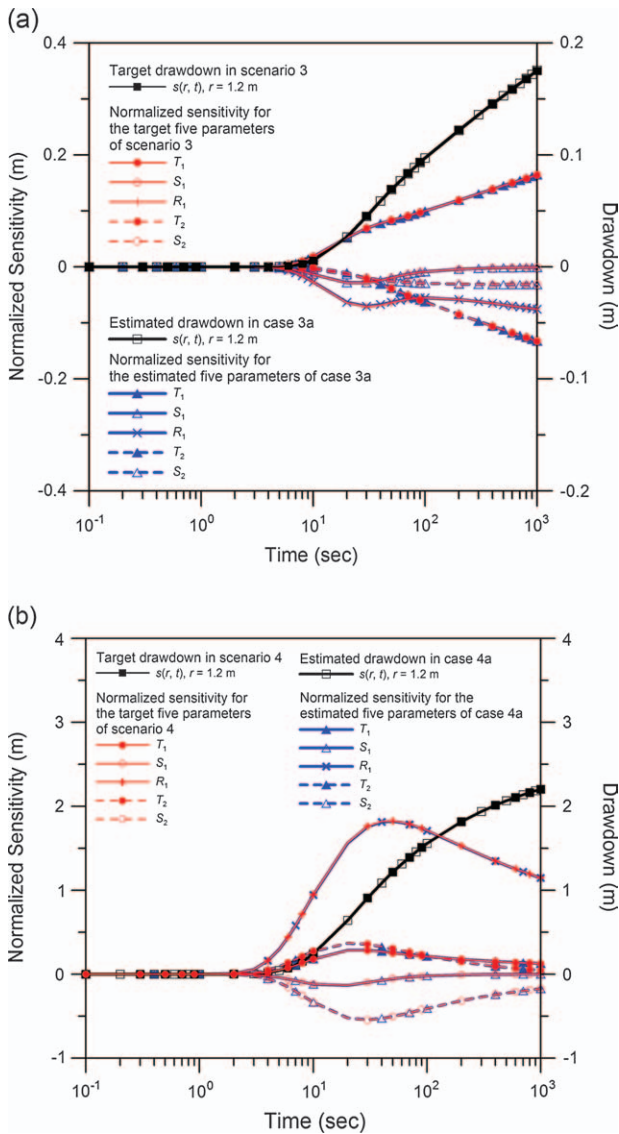|	Estimated Results					
	T_1 (m²/d)	T_2 (m²/d)	S_1	S_2	R_1 (m)	SEE_Q (m³/d)
Target value	0.05	1.0	1.00×10^{-4}	1.00×10^{-4}	0.8	—
1a	0.050	0.718	1.02×10^{-4}	9.91×10^{-4}	0.819	3.19×10^{-3}
1b	0.051	0.908	9.62×10^{-5}	9.89×10^{-4}	0.858	7.49×10^{-3}
1c	0.050	0.795	9.92×10^{-5}	1.00×10^{-5}	0.737	8.68×10^{-3}
1d	0.050	1.321	1.00×10^{-4}	2.05×10^{-4}	0.828	9.05×10^{-3}
1e	0.050	0.868	9.82×10^{-5}	9.85×10^{-4}	0.855	7.02×10^{-3}
Mean	0.050	0.922	9.91×10^{-5}	6.36×10^{-4}	0.819	—
RE (%)	0.32	−7.80	−0.91	535.96	2.41	—
Target value	1.0	0.05	1.00×10^{-4}	1.00×10^{-4}	0.8	—
2a	1.002	0.050	9.93×10^{-5}	9.85×10^{-5}	0.803	2.95×10^{-3}
2b	0.996	0.048	9.89×10^{-5}	1.11×10^{-4}	0.797	3.46×10^{-2}
2c	1.134	0.053	6.39×10^{-5}	5.58×10^{-5}	1.000	5.06×10^{-2}
2d	1.090	0.058	7.32×10^{-5}	4.80×10^{-5}	0.950	4.06×10^{-2}
2e	0.918	0.050	1.30×10^{-4}	1.26×10^{-4}	0.710	3.43×10^{-2}
Mean	1.028	0.052	9.32×10^{-5}	8.79×10^{-5}	0.852	—
RE (%)	2.80	3.63	−6.84	−12.14	6.51	—

except replacing E_1 and M_1 (flow rate data) with E_2 and M_2 (drawdown data), respectively. The time-drawdown curves and normalized sensitivities of the drawdown to the five parameters are displayed in Figure 5a for scenarios 3 and Figure 5b for scenario 4.

The estimated results in scenario 3 show significant deviations on T_1, T_2, S_1, and S_2 with large RE of 679.60%, 678.80%, 730.60%, and 717.60%, respectively. The estimated R_1 has small RE value of −2.40%. In addition, the predicted drawdowns based on the five estimated parameters in scenario 3 are very close to the measured

drawdowns according to the SEE_s values ranging from 2.60×10^{-4} to 1.22×10^{-3} m. As for the negative-skin cases of scenario 4, the accurate estimates for R_1 have small RE values of 0.07%; in contrast, the deviated estimates for T_1, T_2, S_1, and S_2 have large RE of 713.10%, 724.40%, 719.20%, and 723.00%, respectively. Interestingly, in both scenarios 3 and 4, the estimated values for the aquifer diffusivity of the skin and aquifer zones, that is, T_1/S_1 and T_2/S_2, are all close to their target ones. Similar observation was obtained by Hiller and Levy (1994). They demonstrated that only the aquifer diffusivity (T_2/S_2)

Table 2
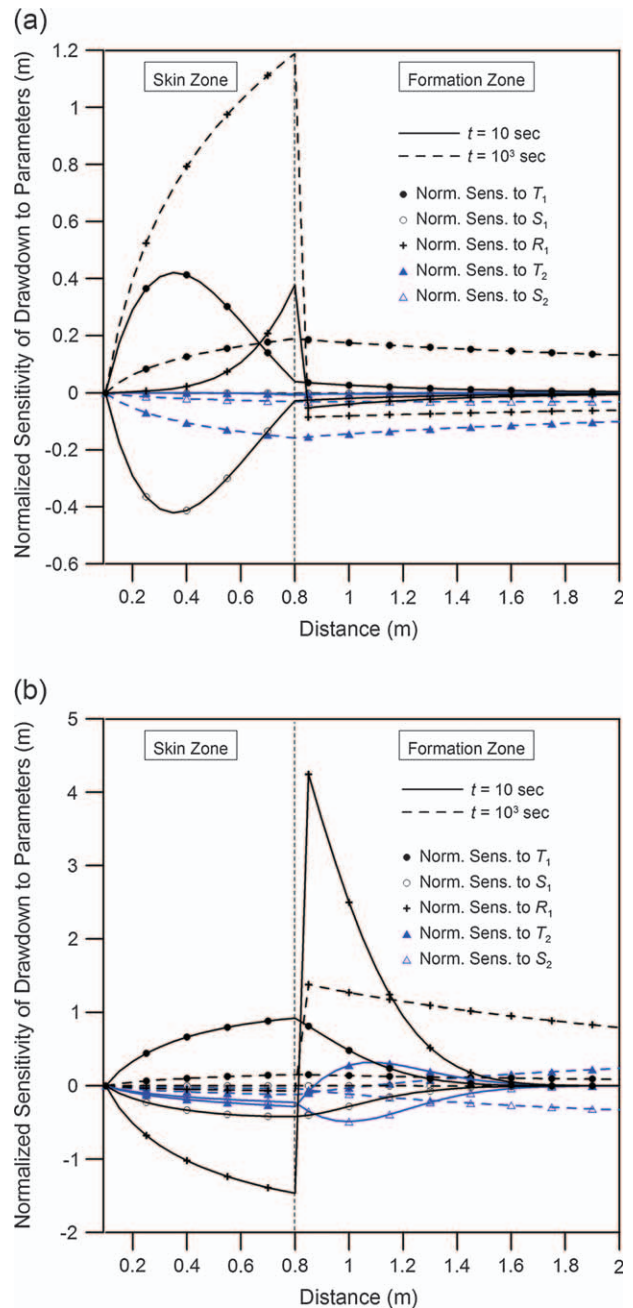**Target Values and Estimated Results for Scenarios 3 and 4**

	Estimated Results							
	T_1 (m²/d)	T_2 (m²/d)	S_1	S_2	R_1 (m)	SEE_s (m)	T_1/S_1 (m²/d)	T_2/S_2 (m²/d)
Target value	0.05	1.0	1.00×10^{-4}	1.00×10^{-4}	0.8	—	5.00×10^{2}	1.00×10^{4}
3a	0.345	6.840	6.88×10^{-4}	7.11×10^{-4}	0.799	2.60×10^{-4}	5.01×10^{2}	9.62×10^{3}
3b	0.362	7.146	7.57×10^{-4}	7.68×10^{-4}	0.786	1.17×10^{-3}	4.78×10^{2}	9.30×10^{3}
3c	0.305	6.902	1.00×10^{-3}	7.06×10^{-4}	0.616	1.07×10^{-3}	3.05×10^{2}	9.78×10^{3}
3d	0.482	9.543	9.83×10^{-4}	9.49×10^{-4}	0.820	9.73×10^{-4}	4.90×10^{2}	1.01×10^{4}
3e	0.455	8.509	7.25×10^{-4}	9.54×10^{-4}	0.883	1.22×10^{-3}	6.28×10^{2}	8.92×10^{3}
Mean	0.390	7.788	8.31×10^{-4}	8.18×10^{-4}	0.781	—	—	—
RE (%)	679.60	678.80	730.60	717.60	−2.40	—	—	—
Target value	1.0	0.05	1.00×10^{-4}	1.00×10^{-4}	0.8	—	1.00×10^{4}	5.00×10^{2}
4a	9.389	0.478	9.50×10^{-4}	9.52×10^{-4}	0.801	3.37×10^{-4}	9.88×10^{3}	5.02×10^{2}
4b	9.933	0.496	9.87×10^{-4}	9.99×10^{-4}	0.801	1.20×10^{-3}	1.01×10^{4}	4.96×10^{2}
4c	5.482	0.268	5.44×10^{-4}	5.35×10^{-4}	0.797	1.05×10^{-3}	1.01×10^{4}	5.01×10^{2}
4d	8.343	0.438	8.65×10^{-4}	8.69×10^{-4}	0.803	9.30×10^{-4}	9.65×10^{3}	5.04×10^{2}
4e	7.508	0.381	7.50×10^{-4}	7.60×10^{-4}	0.801	1.22×10^{-3}	1.00×10^{4}	5.01×10^{2}
Mean	8.131	0.412	8.19×10^{-4}	8.23×10^{-4}	0.801	—	—	—
RE (%)	713.10	724.40	719.20	723.00	0.07	—	—	—

Figure 5. Drawdown curves and the normalized sensitivities to the target and estimated parameters for (a) positive- and (b) negative-skin cases.

Figure 6. Normalized sensitivities of drawdown to the five parameters vs. distance from the test well for (a) positive- and (b) negative-skin cases.

can be estimated when analyzing the late-time drawdown data in the observation well only. Our results indicate that their finding is also applicable to the radial two-zone aquifer system.

Figure 5a shows the time-drawdown curves and the normalized sensitivity curves for drawdown in response to the change in the target and estimated parameters, respectively, in scenario 3 and case 3a. The maximum drawdown during 1000-s CHT is only around 0.175 m, and the insignificant time-drawdown responses in the observation well are also crucial in determining the parameters. The normalized sensitivity curves depict that negative influence on the drawdown occurs when one positively perturbed the skin and aquifer parameters except T_1. The opposite trends of the normalized sensitivity of T_2 to that of T_1 imply a potential difficulty in estimating the parameters. That is, the influence on the drawdown by increasing one parameter may be offset by increasing another.

Figure 5b illustrates the drawdown curve as well as the normalized sensitivities to the changing in the five target parameters used in scenario 4 and those to the five parameters determined from case 4a. The normalized sensitivity curves showing positive perturbations in T_1, R_1, and T_2 produce positive influences on the drawdown, while those in S_1 and S_2 produce negative influences. The normalized sensitivity curves also present high correlation among the parameters, for example, similar patterns between T_1 and T_2 and nearly symmetric patterns of T_1 and T_2 to S_1 and S_2. Although the drawdown response in the observation well in the negative-skin cases is more significant than

that in the positive-skin case, the highly correlated patterns between the parameters T_1, T_2, S_1, and S_2 still cause uncertainties in the parameter estimation. In addition, both Figures 5a and 5b indicate that although the estimated values for T_1, S_1, T_2, and S_2 in cases 3a and 4a are notably different from their target ones, the normalized sensitivity curves to the five estimated parameters are in accordance with those of the five target parameters, respectively. A similar phenomenon may be observed in any other five parameters determined from the analysis of drawdown data measured at the same observation well, for example, those in cases 3b to 3e. Accordingly, T_1, S_1, T_2, and S_2 are difficult to individually identify when only the drawdown data in the observation well are used in the analysis.

Figure 6 illustrates that the patterns of normalized sensitivity at given times are associated with the location of the observation well for the positive- and negative-skin scenarios. Figure 6a shows the difficulties in parameter estimation by only analyzing the drawdown, no matter where the observation well is located. If the observation well is located at the skin zone, the normalized sensitivities to T_1 and S_1 at early time and those to T_1 and T_2 at late time are highly correlated; additionally, the drawdown is insensitive to the change in T_2 at early time, S_1 at late time, and S_2 all the time. If the observation well is located at the aquifer zone, the early-time drawdown seems insensitive to the change in the five parameters; however, the normalized sensitivities of the drawdown to T_1, T_2, and R_1 increase with the test duration. The normalized sensitivity of T_1 at late time shows a symmetric pattern to that of T_2 and causes uncertainties in determining the parameters. In addition, the normalized sensitivities to T_1 and T_2 both slightly decrease with the increasing

distance outside the skin zone. This means, the observation well located far away from the test well also enhances the difficulty in parameter estimation. If the observation well is located at the negative-skin zone, Figure 6b indicates that normalized sensitivities to T_1 and R_1 at early time are symmetric in shape on the horizontal axis and considerably larger than those to other parameters. Similar patterns can be observed within the skin zone from the normalized sensitivity to R_1 at late time and those to T_2 and S_2 all the time; moreover, that of T_1 at late time is opposite to them. If the observation well is located at the aquifer zone, the normalized sensitivities to T_1, S_1, and R_1 all decrease with the distance. Figure 6b also shows that the normalized sensitivity patterns of T_2 and S_2 in the aquifer zone are almost symmetric in time and space, which implies the potential difficulty in determining these two parameters independently.

Parameter Estimation and Sensitivity Analyses Using Specific Drawdown Data

Mishra and Guyonnet (1992) analyzed the specific drawdown responses $(s(r,t)/Q(t))$ in an observation well during a CHT free from the skin effect. Table 3 gives the target values and estimated results from the analysis of specific drawdown data with the presence of a positive skin. In scenario 5, the specific drawdown being analyzed is produced from the measured drawdown given in scenario 1 divided by the wellbore flow rate given in scenario 3. In scenario 6, the case of negative skin, the specific drawdown is produced in a similar way, that is, the drawdown data used in scenario 2 divided by the wellbore flow rate data used in scenario 4. The $SEE_{s/Q}$ values, representing the standard error of the estimated specific drawdown, were calculated using Equation 13 except

Table 3
Target Values and Estimated Results for Scenarios 5 and 6

|			Estimated Results			
	T_1 (m²/d)	T_2 (m²/d)	S_1	S_2	R_1 (m)	$SEE_{s/Q}$ (d/m²)
Target value	0.05	1.0	1.00×10^{-4}	1.00×10^{-4}	0.8	—
5a	0.048	0.987	1.09×10^{-4}	1.03×10^{-4}	0.742	1.73×10^{-3}
5b	0.035	0.966	4.79×10^{-5}	1.14×10^{-4}	1.000	2.22×10^{-3}
5c	0.030	0.969	6.21×10^{-5}	1.09×10^{-4}	0.783	2.18×10^{-3}
5d	0.012	0.984	1.20×10^{-4}	1.02×10^{-4}	0.395	1.94×10^{-3}
5e	0.066	0.998	7.47×10^{-4}	9.85×10^{-5}	0.349	2.52×10^{-3}
Mean	0.038	0.981	2.17×10^{-4}	1.05×10^{-4}	0.654	—
RE (%)	−23.89	−1.91	117.18	5.34	−18.28	—
Target value	1.0	0.05	1.00×10^{-4}	1.00×10^{-4}	0.8	—
6a	7.525	0.055	7.09×10^{-4}	7.05×10^{-5}	0.454	9.43×10^{-3}
6b	7.464	0.057	9.85×10^{-4}	6.45×10^{-5}	0.391	1.09×10^{-2}
6c	4.587	0.057	5.17×10^{-4}	6.32×10^{-5}	0.366	1.04×10^{-2}
6d	1.014	0.053	9.37×10^{-5}	8.08×10^{-5}	0.618	1.54×10^{-2}
6e	1.264	0.048	1.21×10^{-4}	1.13×10^{-4}	0.871	2.16×10^{-2}
Mean	4.371	0.054	4.85×10^{-4}	7.84×10^{-5}	0.540	—
RE (%)	337.07	7.99	385.09	−21.56	−32.53	—

replacing E_1 and M_1 with E_3 and M_3, respectively. Figures 7a and 7b illustrate the normalized sensitivities of the specific drawdown to the five parameters for scenarios 5 and 6, respectively.

For scenario 5, Table 3 shows the accurate estimates of T_2 and S_2 with small RE of −1.91% and 5.34%, respectively. However, slightly deviated estimates of T_1, S_1, and R_1 have RE of −23.89%, 117.18%, and −18.28%, respectively. Cases 5d and 5e show significant deviations in the estimated R_1. Figure 7a shows that the normalized sensitivity plot of T_1 and those of S_1 and R_1 are symmetrical about the horizontal axis, in that they all have a long right-tailed bell shape. The correlation coefficients of each of two parameters' normalized sensitivities for scenarios 5 listed in Table 4 also indicate the highly correlated behavior between the pairs of T_1 and S_1 with the value of −0.998, the pairs of T_1 and R_1 of −0.999, and the pairs of S_1 and R_1 of 0.998. The high-correlated relations for the skin parameters may cause difficulties in estimating their values accurately (Yeh and Chen 2007).

For the negative-skin cases, scenario 6 gives estimated results on T_2 for the mean value of 0.054 m²/d and RE of 7.99% and on S_2 for the mean value of 7.84 × 10^{-5} and RE of −21.56%. Table 4 indicates that the normalized sensitivity of S_2 highly correlates to those of T_2 and R_1 with the correlation coefficients of 0.920 and −0.907, respectively. The estimated skin parameters have large RE of 337.07%, 385.09%, and −32.53% for T_1, S_1, and R_1, respectively. Significantly deviated estimations on the three skin parameters can be observed in cases 6a, 6b, and 6c. Figure 7b shows the symmetric of normalized sensitivities of specific drawdown to the changes in T_1 and S_1 about the horizontal axis. The correlation coefficient of T_1 and S_1, as indicated in Table 4, is −0.794. In addition, the normalized sensitivities of the specific drawdown to the changes in T_1 and R_1 are similar in shape and having a high correlation coefficient of 0.888 for T_1 and R_1. The high correlations between skin parameters in scenario 6 reflect the difficulty in the estimation of the skin parameters from the analysis of specific drawdown data.

Parameter Estimation Using Flow Rate and Drawdown Data Simultaneously

Previous analysis on each of the flow rate, drawdown, and specific drawdown data shows unavoidable flaws in estimating the skin and aquifer parameters. We therefore examined the analysis of the flow rate and drawdown data synchronously in scenarios 7 and 8. The weight w was chosen to be 0.01 d²/m⁴, so that the two objectives, that is, the two sum of squared residuals, were balanced with the same unit and order. Table 5 gives the target values and estimated skin and aquifer parameters of scenarios 7 and 8. The mean values of the estimated results for skin and aquifer parameters are very close to their target values in both scenarios. All RE values are less than 4% with the largest RE in scenarios 7 and 8 both happened on the estimation of S_2. The composite analysis
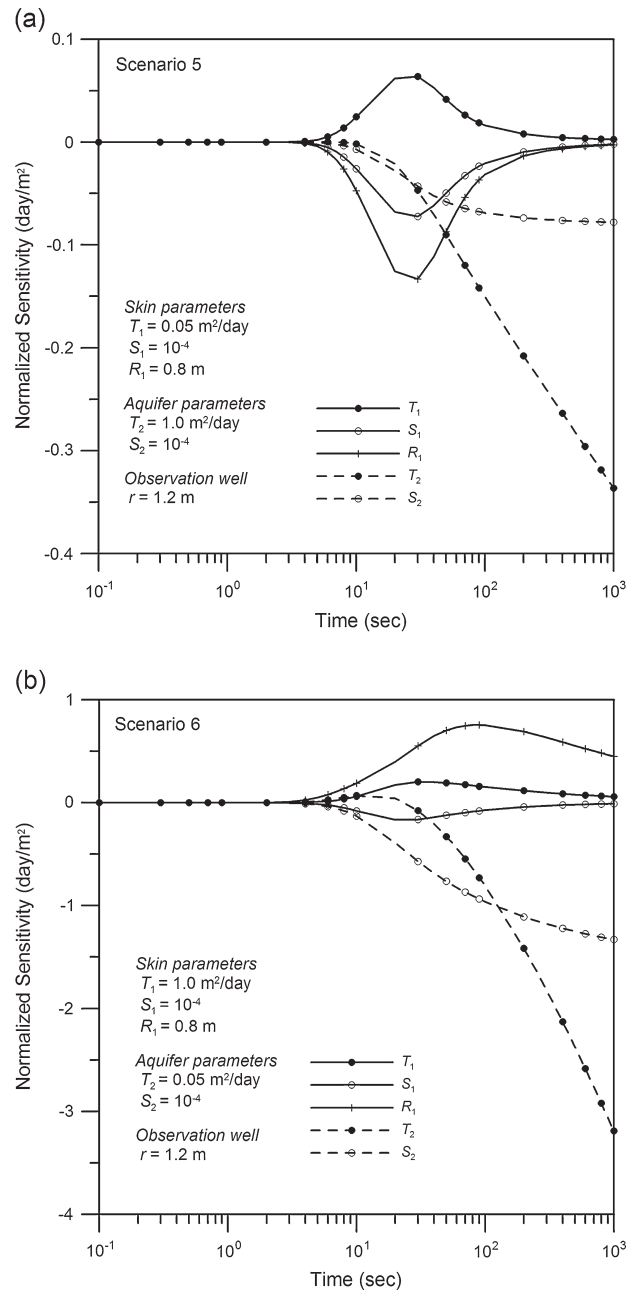
Figure 7. Normalized sensitivities of specific drawdown in response to the change in the five parameters for (a) positive- and (b) negative-skin cases.

of flow rate and drawdown data is highly recommended for improving the accuracy of skin and aquifer parameter estimates.

Conclusions

The CHT data, whether the flow rate at the test well or drawdown responses in the observation well, are affected by the presence of a skin zone. Under this circumstance, the inclusion of the skin effect in the aquifer parameter estimation is inevitable. The sensitivity analysis examines how uncertainties in the skin and aquifer parameters affect the estimated results. The results of sensitivity

Table 4
The Correlation Matrix of Normalized Sensitivities of Specific Drawdown to Parameters for Scenarios 5 and 6

	T_1	T_2	S_1	S_2	R_1
Scenario 5					
T_1	1.000	—	—	—	—
T_2	0.136	1.000	—	—	—
S_1	**−0.998**	−0.122	1.000	—	—
S_2	−0.102	**0.947**	0.127	1.000	—
R_1	**−0.999**	−0.161	**0.998**	0.079	1.000
Scenario 6					
T_1	1.000	—	—	—	—
T_2	−0.340	1.000	—	—	—
S_1	**−0.794**	−0.182	1.000	—	—
S_2	−0.657	**0.920**	0.125	1.000	—
R_1	**0.888**	−0.671	−0.453	**−0.907**	1.000

analyses and parameter estimations provide valuable references in analyzing the skin-affected CHT data.

Major conclusions are summarized subsequently. First, the sensitivity analysis reveals that the changes in aquifer parameters cause little impact on the flow rate, especially in the positive-skin cases. That is, aquifer information behind the flow rate data may be overshadowed by the skin effect. As a result, analysis of the flow rate data at the test well only may yield good estimates for the skin parameters yet less reliable estimates for the aquifer parameters. It is therefore suggested to analyze the flow rate data if the skin zone parameters are particularly of interest. Next, for both positive- and negative-skin cases, the sensitivities of drawdown to parameters showed highly correlated relations that may cause uncertainties in the parameter estimation. Another difficulty in the parameter estimation happened in the positive-skin cases can be attributed to the insignificant drawdown response in the observation well throughout the CHT duration. The sensitivity plots demonstrated that different sets of the five parameters could produce identical sensitivity patterns as long as the same values of the skin and aquifer diffusivities and the outer radius of skin zone were applied. It is therefore hard to obtain accurate estimates for the transmissivity and storativity for each of skin and aquifer zones from the analysis of the drawdown

Table 5
Target Values and Estimated Results for Scenarios 7 and 8

	T_1 (m²/d)	T_2 (m²/d)	S_1	S_2	R_1 (m)	SEE_Q (m³/d)	SEE_s (m)
	Estimated Results						
Target value	0.05	1.0	1.00×10^{-4}	1.00×10^{-4}	0.8	—	—
7a	0.050	0.994	1.02×10^{-4}	1.01×10^{-4}	0.788	3.25×10^{-3}	2.66×10^{-4}
7b	0.051	0.974	9.53×10^{-5}	1.08×10^{-4}	0.828	7.58×10^{-3}	1.17×10^{-3}
7c	0.050	0.998	1.01×10^{-4}	1.01×10^{-4}	0.793	8.92×10^{-3}	1.09×10^{-3}
7d	0.050	0.983	9.92×10^{-5}	1.04×10^{-4}	0.816	9.24×10^{-3}	9.94×10^{-4}
7e	0.050	0.994	9.96×10^{-5}	1.04×10^{-4}	0.797	7.22×10^{-3}	1.23×10^{-3}
Mean	0.050	0.989	9.94×10^{-5}	1.04×10^{-4}	0.804	—	—
RE (%)	0.40	−1.14	−0.58	3.60	0.55	—	—
Target value	1.0	0.05	1.00×10^{-4}	1.00×10^{-4}	0.8	—	—
8a	0.999	0.050	1.00×10^{-4}	9.97×10^{-5}	0.800	3.05×10^{-3}	3.55×10^{-4}
8b	0.997	0.050	9.85×10^{-5}	1.01×10^{-4}	0.802	3.50×10^{-2}	1.22×10^{-3}
8c	0.991	0.050	1.03×10^{-4}	9.74×10^{-5}	0.797	5.92×10^{-2}	1.19×10^{-3}
8d	0.989	0.049	1.03×10^{-4}	9.63×10^{-5}	0.796	5.32×10^{-2}	1.30×10^{-3}
8e	0.996	0.050	1.01×10^{-4}	9.99×10^{-5}	0.800	3.75×10^{-2}	1.25×10^{-3}
Mean	0.994	0.050	1.01×10^{-4}	9.89×10^{-5}	0.799	—	—
RE (%)	−0.57	−0.24	1.10	−1.14	−0.15	—	—

data only. The estimates for the five parameters showed that the use of SA procedure in the data analysis can accurately estimate the skin and aquifer diffusivities and the thickness of the skin zone. Furthermore, the normalized sensitivities of specific drawdown showed highly correlated relations among the skin zone parameters. This may cause difficulties in accurately estimating the values of skin zone parameters; however, the specific drawdown data can still be used to determine the aquifer parameters even if the CHT is affected by the skin effect. Finally, it is highly recommended adopting the flow rate and drawdown data simultaneously for the CHT data analysis because their estimates for the skin and aquifer parameters are the most accurate among the four suites of CHT data analyses.

Acknowledgments

References

Aarts, E., and J. Korst. 1989. *Simulated Annealing and Boltzmann Machines: A Stochastic Approach to Combinatorial Optimization and Neural Computing*. New York: John Wiley and Sons.

Chang, Y.C., H.D. Yeh, and Y.C. Huang. 2008. Determination of the parameter pattern and values for a one-dimensional multi-zone unconfined aquifer. *Hydrogeology Journal* 16, no. 2: 205–214, doi:10.1007/s10040-007-0228-3.

Chen, C.S., and C.C. Chang. 2003. Well hydraulics theory and data analysis of the constant-head test in an unconfined aquifer with the skin effect. *Water Resources Research* 39, no. 5: 1121, doi:10.1029/2002WR001516.

Cooper, H.H., and C.E. Jacob. 1946. A generalized graphical method for evaluating formation constants and summarizing well field history. *Transactions of the American Geophysical Union* 27, no. 4: 526–534.

Corana, A., M. Marchesi, C. Martini, and S. Ridella. 1987. Minimizing multimodal functions of continuous variables with the "simulated annealing" algorithm. *ACM Transactions on Mathematical Software* 13, no. 3: 262–280.

Cunha, M.D.C., and J. Sousa. 1999. Water distribution network design optimization: Simulated annealing approach. *Journal of Water Resources Planning and Management* 125, no. 4: 215–221.

Dougherty, D.E., and R.A. Marryott. 1991. Optimal groundwater management. 1. Simulated annealing. *Water Resources Research* 27, no. 10: 2493–2508.

Hantush, M.S. 1964. Hydraulics of wells. In *Advances in Hydroscience*, vol. 1, ed. V.T. Chow, 281–442. New York: Academic Press.

Hiller, C.K., and B.S. Levy. 1994. Estimation of aquifer diffusivity from analysis of constant-head pumping test data. *Ground Water* 32, no. 1: 47–52.

Huang, Y.C., and H.D. Yeh. 2007. The use of sensitivity analysis in on-line aquifer parameter estimation. *Journal of Hydrology* 335, no. 3–4: 406–418.

IMSL. 2003a. *IMSL Fortran Library User's Guide Math/Library Volume 2 of 2, version 5.0*. Houston, Texas: Visual Numerics.

IMSL. 2003b. *IMSL Fortran Library User's Guide Stat/Library Volume 2 of 2, version 5.0*. Houston, Texas: Visual Numerics.

Jacob, C.E., and S.W. Lohman. 1952. Nonsteady flow to a well of constant drawdown in an extensive aquifer. *Transactions of the American Geophysical Union* 33, no. 4: 559–569.

Jiao, J.J., and K.R. Rushton. 1995. Sensitivity of drawdown to parameters and its influence on parameter estimation for pumping tests in large-diameter wells. *Ground Water* 33, no. 5: 794–800.

Kabala, Z.J. 2001. Sensitivity analysis of a pumping test on a well with wellbore storage and skin. *Advances in Water Resources* 24, no. 5: 483–504.

Kirkpatrick, S., C.D. Gelatt Jr., and M.P. Vecchi. 1983. Optimization by simulated annealing. *Science* 220, no. 4598: 671–680.

Kuo, S.F., C.W. Liu, and G.P. Merkley. 2001. Application of the simulated annealing method to agricultural water resource management. *Journal of Agricultural Engineering Research* 80, no. 1: 109–124.

Leng, C.H., and H.D. Yeh. 2003. Aquifer parameter identification using the extended Kalman filter. *Water Resources Research* 39, no. 3: 1062, doi:10.1029/2001WR000840.

Lin, Y.C., and H.D. Yeh. 2005. Trihalomethane species forecast using optimization method: Genetic algorithm and simulated annealing. *Journal of Computing in Civil Engineering* 19, no. 3: 248–257.

Marryott, R.A., D.E. Dougherty, and R.L. Stollar. 1993. Optimal groundwater management. 2. Application of simulated annealing to a field-scale contamination site. *Water Resources Research* 29, no. 4: 847–860.

McElwee, C.D., and M.A. Yukler. 1978. Sensitivity of groundwater models with respect to variations in transmissivity and storage. *Water Resources Research* 14, no. 3: 451–459.

Metropolis, N., A.W. Rosenbluth, M.N. Rosenbluth, A.H. Teller, and E. Teller. 1953. Equation of state calculations by fast computing machines. *Journal of Chemical Physics* 21, no. 6: 1087–1092.

Mishra, S., and D. Guyonnet. 1992. Analysis of observation-well response during constant-head testing. *Ground Water* 30, no. 4: 523–528.

Peng, H.Y., H.D. Yeh, and S.Y. Yang. 2002. Improved numerical evaluation for the radial groundwater flow equation. *Advances in Water Resources* 25, no. 6: 663–675.

Theis, C.V. 1935. The relation between the lowering of the piezometric surface and the rate and duration of discharge of a well using groundwater storage. *Transactions of the American Geophysical Union* 16, no. 2: 519–524.

Yang, S.Y., and H.D. Yeh. 2006. A novel analytical solution for constant-head test in a patchy aquifer. *International Journal for Numerical and Analytical Methods in Geomechanics* 30, no. 12: 1213–1230.

Yang, S.Y., and H.D. Yeh. 2005. Laplace-domain solutions for radial two-zone flow equations under the conditions of constant-head and partially penetrating well. *Journal of Hydraulic Engineering* 131, no. 3: 209–216.

Yang, S.Y., and H.D. Yeh. 2002. Solution for flow rates across the wellbore in a two-zone confined aquifer. *Journal of Hydraulic Engineering* 128, no. 2: 175–183.

Yeh, H.D. 1987. Theis' solution by nonlinear least-squares and finite-difference Newton's method. *Ground Water* 25, no. 6: 710–715.

Yeh, H.D., and Y.C. Lin. 2008. Pipe network system analysis using simulated annealing. *Journal of Water Supply: Research and Technology – AQUA* 57, no. 5: 317–327.

Yeh, H.D., and Y.J. Chen. 2007. Determination of skin and aqui-
fer parameters for a slug test with wellbore-skin effect.
Journal of Hydrology 342, no. 3–4: 283–294.
Yeh, H.D., T.H. Chang, and Y.C. Lin. 2007a. Groundwater con-
taminant source identification by a hybrid heuristic
approach. *Water Resources Research* 43, no. 9: W09420,
doi:10.1029/2005WR004731.
Yeh, H.D., Y.C. Lin, and Y.C. Huang. 2007b. Parameter identifi-
cation for leaky aquifers using global optimization meth-
ods. *Hydrological Processes* 21, no. 7: 862–872.
Zheng, C., and P. Wang. 1996. Parameter structure identification
using tabu search and simulated annealing. *Advances in
Water Resources* 19, no. 4: 215–224.

Appendix A

The Mathematical Model of Yang and Yeh (2002)

Yang and Yeh (2002) considered a CHT conducted in
a homogeneous, isotropic, infinite extent, and confined
aquifer. The test well was fully penetrating with a finite
radius. The ground water flow system was characterized
as a radial two-zone system with a finite thickness skin
zone surrounding the test well. They gave the flow equa-
tions in the skin and aquifer zones, respectively, as

$$\frac{\partial^2 s_1}{\partial r^2} + \frac{1}{r}\frac{\partial s_1}{\partial r} = \frac{S_1}{T_1}\frac{\partial s_1}{\partial t}, \quad r_w \leq r \leq R_1 \quad (A1)$$

$$\frac{\partial^2 s_2}{\partial r^2} + \frac{1}{r}\frac{\partial s_2}{\partial r} = \frac{S_2}{T_2}\frac{\partial s_2}{\partial t}, \quad R_1 < r < \infty \quad (A2)$$

subject to the following initial and boundary conditions

$$s_1(r,0) = s_2(r,0) = 0, \quad r > r_w \quad (A3)$$

$$s_1(r_w,t) = s_w, \quad t > 0 \quad (A4)$$

$$s_2(\infty,t) = 0 \quad (A5)$$

$$s_1(R_1,t) = s_2(R_1,t) \quad (A6)$$

$$T_1\frac{\partial s_1(R_1,t)}{\partial r} = T_2\frac{\partial s_2(R_1,t)}{\partial r} \quad (A7)$$

Equations A1 through A7 were solved by the Laplace
transform and the Bromwich integral. The Laplace-
domain drawdown solutions in the skin and aquifer zones
are given as Equations 4 and 5, respectively. The flow rate
solution was obtained applying Darcy's law to Equation 4.

Appendix B

Notation List

The following symbols are used in this article:

E_k	kth type of model predicted CHT data
f_k	Objective function of the kth type of CHT data
I_0, I_1	Modified Bessel function of the first kind of order 0 and 1, respectively
K_0, K_1	Modified Bessel function of the second kind of order 0 and 1, respectively
M_k	The k_{th} type of measured field data
O_i	Model output quantities at time i
p	Laplace variable
P	Acceptance probability used in SA
P_k	kth model input parameter
$\underline{p_e}$	Parameter vector
q_1	$\sqrt{pS_1/T_1}$
q_2	$\sqrt{pS_2/T_2}$
Q_m	Flow rate data with the measurement error
Q_{ub}	Noise-free flow rate data
$\overline{Q}$	Flow rate across the wellbore in the Laplace domain
r	Radial distance from test well to observation well
r_w	Radius of test well
R_1	Radial distance from test well to outer boundary of skin zone
RE	Relative error
RN	Random number
s_1, s_2	Drawdown responses in the skin and aquifer zone, respectively
$\overline{s}_1, \overline{s}_2$	Laplace-domain drawdown responses in the skin and aquifer zone, respectively
s_m	Drawdown data with the measurement error
s_{ub}	Noise-free drawdown data
s_w	Constant drawdown maintained at the well during the test
S_1, S_2	Storativity of skin and aquifer zone, respectively
SEE$_Q$	Standard error of estimate for the flow rate data
SEE$_s$	Standard error of estimate for the drawdown data
SEE$_{s/Q}$	Standard error of estimate for the specific drawdown data
t	Test time
T	System temperature used in SA
T_1, T_2	Transmissivity of skin and aquifer zone, respectively
v	Degree of freedom
$X_{i,k}$	Normalized sensitivity of kth input parameter at time i
ε	Magnitude of error
ΔP_k	Small increment of kth model input parameter
Φ_1	$\sqrt{\frac{S_2 T_2}{S_1 T_1}}K_0(q_1R_1)K_1(q_2R_1) - K_1(q_1R_1)K_0(q_2R_1)$
Φ_2	$\sqrt{\frac{S_2 T_2}{S_1 T_1}}I_0(q_1R_1)K_1(q_2R_1) + I_1(q_1R_1)K_0(q_2R_1)$
$\underline{\Omega}$	Solution space vector